International Journal of Industrial Engineering & Production Research June 2023 Vol. 34, No. 2: 1-17
DOI: 10.22068/ijiepr.34.2.12

RESEARCH PAPER

A Ridge Penalized Likelihood Ratio Chart for Phase II Monitoring of High-Dimensional Process Dispersion Under Measurement System Inaccuracy

Esmaeil Safikhani[1], Ali Salmasnia[2*] & Mohammad Reza Maleki[3]

Received 30 April 2022; Revised 20 May 2023; Accepted 27 May 2023;

ABSTRACT

In some applications, the number of quality characteristics is larger than the number of observations within subgroups. Common multivariate control charts to monitor the variability of such high-dimensional processes are unsuitable because the sample covariance matrix is not positive semi-definite and invertible. Moreover, the impact of gauge imprecision on detection capability of multivariate control charts under high-dimensional setting has been clearly neglected in the literature. To overcome these shortcomings, this paper develops a ridge penalized likelihood ratio chart for Phase II monitoring of high-dimensional process in the presence of measurement system errors. The developed control chart departures from the assumption of sparse variability shifts in which the assignable cause can only affect a few elements of the covariance matrix. Then, to compensate for the adverse impact of gauge impression, the developed chart is extended by employing multiple measurements on each sampled item. Simulation studies are carried out to study the impact of imprecise measurements on detectability of the developed monitoring scheme under different shift patterns. The results show that the gauge inability negatively affects the run-length distribution of the developed control chart. It is also found that the extended chart under multiple measurements strategy can effectively reduce the error impact.

KEYWORDS: *High-dimensional process; Covariance matrix; Measurement errors; Ridge penalized likelihood ratio statistic; Multiple measurements per item.*

1. Introduction

In today's competitive markets, companies are increasingly focusing on a large number of process quality characteristics to keep their market share, enhance customer satisfaction, and keep ahead of competition. Fortunately, the recent advances in data acquisition technologies have provided the possibility of collecting a great deal of information regarding quality characteristics of interest. On the other hand, data analysis obtained from each sample in processes with a large number of quality characteristics entails a considerable amount of time and cost. In such situation, taking large samples has two main drawbacks: (1) it imposes a severe cost on manufacturer; (2) in manufacturing systems with low production speed, it is not possible to wait until a sufficient sample size be collected. Consequently, the quality practicians may face conditions in which the number of process quality characteristics is larger than the sample size called "high-dimensionality". In this regard, [1] developed an improved version of the generalized T^2 chart based on random matrix theory for Phase II monitoring of high-dimensional; process mean. [2] integrated a divide-and-conquer strategy and multivariate exponentially weighted moving average (MEWMA) statistic for monitoring high-dimensional processes in which normality assumption of quality characteristics is relaxed

* Corresponding author: *Ali Salmasnia*
a.salmasnia@qom.ac.ir

1. *Department of Industrial Engineering, University of Eyvanekey, Semnan, Iran.*
2. *Department of Industrial Engineering, Faculty of Engineering, University of Qom, Iran.*
3. *Industrial Engineering Group, Golpayegan College of Engineering, Isfahan University of Technology, Golpayegan 87717-67498, Iran.*

[3] presented an integrated monitoring and diagnosis method based on principal component analysis (PCA) for high-dimensional data streams.

Using commonplace control charts to monitor the variability of high-dimensional processes is challenging because the sample covariance matrix is not positive semi-definite and its determinant tends toward zero. To overcome this problem, [4] proposed a novel algorithm based on parallelized Monte-Carlo simulation to enhance the sensitivity of two memory-type control charts for monitoring the variability of high dimensional processes. They employed different techniques for decreasing the computing space and run time. An adaptive LASSO-thresholding-based control chart for Phase II monitoring of multivariate normal quality characteristics under high-dimensional setting was suggested by [5] suggested. Using different out-of-control patterns, they confirmed the superiority of their proposed control chart over existing control charts. In contrast to the above-mentioned studies, [6] focused on detection of general changes in covariance matrix elements without sparsity assumption in Phase II monitoring of high-dimensional process variability. [7] extended the LASSO-thresholding-based control chart for Phase I monitoring of multivariate processes in condition that the process dimension is larger than the sample size. Using a real industrial data from the process of spur gear production, they validated the applicability of their proposed control chart. [8] gave the idea of tracking changes in sparse leading eigenvalue between two covariance matrices and studied Phase I monitoring high-dimensional process variability. [9] integrated ridge penalized likelihood ratio (RPLR) statistic and multiple dependent state sampling (MDS) strategy for monitoring high-dimensional covariance matrices. Then, they presented an improved version of the developed monitoring scheme based on generalized multiple dependent state sampling. The adverse effect of gauge inaccuracy on the performance of the adaptive thresholding LASSO control charting method for monitoring high-dimensional process variability was evaluated by [10]. They showed that the developed charting method has a better performance than the entropy chart in both with and without measurement error conditions. [11] equipped the adaptive thresholding LASSO chart with double sampling (DS) strategy for improving the chart sensitivity in reacting to deviations of covariance matrix elements from their nominal values.

A vital issue affecting the performance of multivariate control charts is the ability of measurement system to accurately measure the quality characteristics of interest. Although some sources of uncertainty caused by the measurement devices always exist in reality, most existing control charts have been established based on the assumption of precise measurements. The existence of measurement error which is defined as the difference between the accurate and measured values of the process quality characteristics can significantly affects the performance of control charts. Consequently, it is crucial to develop the chart statistic by: (1) taking the measurement error component into account; (2) employing remedial strategies to reduce the impact of measurement inaccuracy on chart performance. Fortunately, the impact of measurement errors on detection capability of control charts have been well documented by recent studies such as [12-17]. More specifically, in the context of multivariate control charts, [18] used a linearly covariate error model and probed the impact of imprecise measurements on sensitivity of the variable sampling intervals (VSI) Hotelling's T^2 control chart. The impact of gauge measurement errors using a linear covariate model on the performance of the Hotelling CoDa (Compositional Data) T^2 control chart was studied by [19-20] studied the influence of gauge measurement errors on the performance of some one-sided variable sampling interval (VSI) EWMA-based control charts to monitor the multivariate coefficient of variation. More studies can be found in [21-25]. Interested readers can refer to review paper provided by [26].

This paper proposes a ridge penalized likelihood ratio chart with five important features: (1) it can be employed to monitor multivariate process variability when the process dimension exceeds the sample size; (2) it departures from the assumption of sparse in-control covariance matrix; (3) in contrast to the existing charts for monitoring high-dimensional process variability that are only applicable for sparse changes, it can be used for detecting general shift patterns in the original variability matrix; (4) it takes the existence of gauge imprecision into account; and (5) it develops multiple measurements strategy to compensate for the undesired impact of error variance on chart performance. Note that, sparce variability changes is referred to condition that

only few covariance matrix elements are simultaneously effected by assignable.

The structure of this paper is organized as follows: The ridge penalized likelihood ratio statistic considering an additive covariate model is developed in Section 2. To reduce the undesired impact of contaminated data due to gauge impression, the developed chart is extended on the basis of multiple measurements strategy in Section 3. Simulation studies in terms of run length properties are conducted in Section 4 to compare the detection capability of the ridge penalized likelihood ratio chart under with and without errors scenarios. Ultimately, Section 5 furnishes the conclusions of our proposed charts and provides some recommendations for future studies.

2. RPLRME Control Chart

In this section, a control chart for Phase II monitoring of high-dimensional process variability is developed based on the ridge penalized likelihood ratio statistic under the gauge measurement errors. The developed chart hereafter called RPLRME chart has the following advantages: (1) considering general covariance matrix shift patterns without the sparsity assumption, (2) detecting covariance matrix abnormalities even when the process dimension exceed the subgroup size, (3) taking into account the gauge inability to accurately measure the value of process quality characteristics, and (4) presenting a closed from to estimate the precision matrix in contrast to the conventional penalized likelihood ratio-based charts which suffer from complex computational procedures. In this regard, first the variables and parameters used to establish the RPLRME chart are summarized in Table 1.

Tab. 1. Notations

Notation	Description
Indices	
t	Index of subgroups
i	Index of observations
j,k	Index of quality characteristics
r	Index of measurements per item
Distribution parameters	
$\mathbf{X}_t$	Accurate values matrix of observations in subgroup t
$\mathbf{x}_{ti}$	i^{th} observation vector of quality characteristics in subgroup t
x_{tjk}	i^{th} observation of j^{th} quality characteristic in subgroup t
p	Number of quality characteristics
$\boldsymbol{\mu}_{\mathbf{X}}$	Mean vector of $\mathbf{X}_t$
$\boldsymbol{\Sigma}_{\mathbf{X}}$	Covariance matrix of $\mathbf{X}_t$
$\boldsymbol{\Sigma}_{\mathbf{X},ic}$	In-control covariance matrix of $\mathbf{X}_t$
$\boldsymbol{\Sigma}_{\mathbf{X},oc}$	Out-of-control covariance matrix of $\mathbf{X}_t$
σ_{jk}	Covariance of quality characteristics j and k
σ_j^2	Variance of j^{th} quality characteristic
Chart parameters	
α	Probability of Type I error
n	Sample size
θ	Tuning parameter
$RPLRME$	Statistic of ridge penalized likelihood ratio with measurement errors
$RPLRMME$	Statistic of ridge penalized likelihood ratio under multiple measurements
UCL_{RPLRME}	Upper control limit of RPLRME chart
$UCL_{RPLRMME}$	Upper control limit of RPLRMME chart

Error parameters	
$\boldsymbol{\varepsilon}_t$	Error terms matrix in subgroup t
$\boldsymbol{\varepsilon}_{ti}$	The i^{th} column of $\boldsymbol{\varepsilon}_t$
$\boldsymbol{\mu}_{\boldsymbol{\varepsilon}}$	Mean vector of $\boldsymbol{\varepsilon}_{ij}$
$\boldsymbol{\Sigma}_{\boldsymbol{\varepsilon}}$	Covariance matrix of $\boldsymbol{\varepsilon}_{ij}$
$\sigma^2_{\varepsilon,j}$	Variance of error term related to quality characteristic j
$\mathbf{A}$	Intercept coefficients vector of multivariate additive covariate model
$\mathbf{B}$	Slope coefficients vector of multivariate additive covariate model
$\mathbf{Y}_t$	Measured values matrix of observations in subgroup t
$\boldsymbol{\mu}_{\mathbf{Y}} = \mathbf{A} + \mathbf{B}\boldsymbol{\mu}_{\mathbf{X}}$	Mean vector of $\mathbf{Y}_t$
$\boldsymbol{\Sigma}_{\mathbf{Y}} = \mathbf{B}\boldsymbol{\Sigma}_{\mathbf{X}}\mathbf{B}^T + \boldsymbol{\Sigma}_{\boldsymbol{\varepsilon}}$	Covariance matrix of $\mathbf{Y}_t$
$\boldsymbol{\Sigma}_{\mathbf{Y},ic}$	In-control covariance matrix of $\mathbf{Y}_t$
$\boldsymbol{\Omega}$	Precision matrix of $\mathbf{Y}_t$
$\boldsymbol{\Omega}_{ic}$	In-control precision matrix of $\mathbf{Y}_t$
$\boldsymbol{\Omega}^m_{ic}$	In-control precision matrix of $\bar{\mathbf{Y}}_t$
$\hat{\boldsymbol{\Omega}}^{MLE}_t$	Estimated precision matrix of $\mathbf{Y}_t$ based on MLE
$\hat{\boldsymbol{\Omega}}^{RPLRME}_t$	Estimated precision matrix of $\mathbf{Y}_t$ based on RPLRME
$\hat{\boldsymbol{\Omega}}^{RPLRMME}_t$	Estimated precision matrix of $\bar{\mathbf{Y}}_t$ based on RPLRMME
m	Number of measurements on a given item
Others	
$\mathbf{S}_t$	Sample covariance matrix in subgroup t
$\mathbf{S}^m_t$	Sample covariance matrix in subgroup t under multiple measurements per item
ARL_{ic}	In-control average run length
ARL_{oc}	Out-of-control average run length
$SDRL_{ic}$	In-control standard deviation of run length
$SDRL_{oc}$	Out-of-control standard deviation of run length
τ	Sampling interval in which an assignable cause occurs
T	Sampling interval in which the chart signals an out-of-control signal

Let $\mathbf{X}_t = (\mathbf{x}_{t1}, \mathbf{x}_{t2}, ..., \mathbf{x}_{tn})_{p\times n}; t = 1,2,...,T$ be a $p \times n$ matrix of observations collected at t^{th} sampling point in which the i^{th} observation denoted as $\mathbf{x}_{ti} = \left(x_{tj1}, x_{tj2}, ..., x_{tjp}\right)^T; i = 1,...,n$ follows a p-variate normal distribution. The occurrence of assignable causes at sampling point τ changes the process covariance matrix from $\boldsymbol{\Sigma}^{ic}_{\mathbf{X}}$ to $\boldsymbol{\Sigma}^{oc}_{\mathbf{X}}$. In fact, for subgroups $t = 1,2,...,\tau$, the process parameters remain in-control i.e., $\mathbf{x}_{ti} \sim MVN(\boldsymbol{\mu}_{\mathbf{X}}, \boldsymbol{\Sigma}^{ic}_{\mathbf{X}})$ whereas we have $\mathbf{x}_{ti} \sim MVN(\boldsymbol{\mu}_{\mathbf{X}}, \boldsymbol{\Sigma}^{oc}_{\mathbf{X}})$ at sampling points $t = \tau + 1,...,T$. In this study, we consider an additive covariate model to associate the accurate values of quality characteristics with their corresponding measured values as:

$$\mathbf{Y}_t = \mathbf{A} + \mathbf{B}\mathbf{X}_t + \boldsymbol{\varepsilon}_t \quad (1)$$

where $\mathbf{Y}_t = (\mathbf{y}_{t1}, \mathbf{y}_{t2}, ..., \mathbf{y}_{tn})_{p\times n}$ denotes the matrix of measured quality characteristics at t^{th} sampling stage while $\mathbf{A} = \left(a_1, a_2, ..., a_p\right)^T$ and $\mathbf{B} = \begin{pmatrix} b_1 & 0 & \dots & 0 \\ 0 & b_2 & \dots & 0 \\ \vdots & \vdots & \ddots & \vdots \\ 0 & 0 & \cdots & b_p \end{pmatrix}_{p\times p}$ contain constant intercept and slope error model parameters, respectively. Moreover, $\boldsymbol{\varepsilon}_t = (\boldsymbol{\varepsilon}_{t1}, \boldsymbol{\varepsilon}_{t2}, ..., \boldsymbol{\varepsilon}_{tn})_{p\times n}$ represents the matrix of error values which follows a p-variate normal distribution with parameters $\boldsymbol{\mu}_{\boldsymbol{\varepsilon}} = (0, 0, ..., 0)^T$, $\boldsymbol{\Sigma}_{\boldsymbol{\varepsilon}} = \begin{pmatrix} \sigma^2_{\varepsilon,1} & 0 & \dots & 0 \\ 0 & \sigma^2_{\varepsilon,2} & \dots & 0 \\ \vdots & \vdots & \ddots & \vdots \\ 0 & 0 & \dots & \sigma^2_{\varepsilon,p} \end{pmatrix}$ and is independent from $\mathbf{X}_t$. According to Equation (1), $\mathbf{y}_{ti}; i = 1, ..., n$ follows a p-variate normal distribution with mean vector $\boldsymbol{\mu}_{\mathbf{Y}}$ and covariance matrix $\boldsymbol{\Sigma}_{\mathbf{Y}}$ as:

$$\boldsymbol{\mu}_{\mathbf{Y}} = \mathbf{A} + \mathbf{B}\boldsymbol{\mu}_{\mathbf{X}} \quad (2)$$

$$\boldsymbol{\Sigma}_{\mathbf{Y}} = \mathbf{B}\boldsymbol{\Sigma}_{\mathbf{X}}\mathbf{B}^T + \boldsymbol{\Sigma}_{\boldsymbol{\varepsilon}} = \begin{pmatrix} b_1^2\sigma_1^2 + \sigma^2_{\varepsilon,1} & b_1 b_2 \sigma_{12} & \dots & b_1 b_p \sigma_{1p} \\ b_2 b_1 \sigma_{12} & b_2^2\sigma_2^2 + \sigma^2_{\varepsilon,2} & \dots & b_2 b_p \sigma_{2p} \\ \vdots & \vdots & \ddots & \vdots \\ b_p b_1 \sigma_{1p} & b_2 b_p \sigma_{2p} & \dots & b_p^2\sigma_p^2 + \sigma^2_{\varepsilon,p} \end{pmatrix}_{p\times p} \quad (3)$$

In order to estimate the precision matrix $\boldsymbol{\Omega}$, the likelihood function at t^{th} sampling stage given the vectors $\mathbf{y}_{t1}, \mathbf{y}_{t2}, ..., \mathbf{y}_{tn}$ is constructed as:

$$f(\mathbf{y}_{t1}, ..., \mathbf{y}_{tn} | \boldsymbol{\Omega}) = (2\pi n)^{\frac{-p}{2}} |\boldsymbol{\Omega}|^{\frac{1}{2}} e^{-\sum_{i=1}^{n}(\mathbf{y}_{ti}-\boldsymbol{\mu}_Y)^T \boldsymbol{\Omega} (\mathbf{y}_{ti}-\boldsymbol{\mu}_Y)} \quad (4)$$

where $\boldsymbol{\Omega} = \boldsymbol{\Sigma}_{\mathbf{Y}}^{-1}$. The maximum likelihood estimator (MLE) of precision matrix can be estimated by solving the optimization problem as below:

$$\hat{\boldsymbol{\Omega}}_t^{MLE} = \arg\min_{\boldsymbol{\Omega}} \left\{ tr(\boldsymbol{\Omega}\mathbf{S}_t) - \log|\boldsymbol{\Omega}| \right\} \quad (5)$$

where $\mathbf{S}_t = \frac{1}{n}\sum_{i=1}^{n}(\mathbf{y}_{ti} - \boldsymbol{\mu}_Y)(\mathbf{y}_{ti} - \boldsymbol{\mu}_Y)^T$ denotes the sample covariance matrix for t^{th} random subgroup. For sampling stage $t; t = 1, ..., T$, the optimum solution of the mathematical programming (5) will be equal to the inverse of the sample covariance matrix as $\hat{\boldsymbol{\Omega}}_t^{MLE} = \mathbf{S}_t^{-1}$. However, using MLE approach to estimate the precision matrix is inapplicable when p is larger than n because $\mathbf{S}_t$ is not invertible. For two reasons of: (1) shrinking the unchanged elements in $\boldsymbol{\Sigma}_{\mathbf{Y}}$ to the corresponding ones in $\boldsymbol{\Sigma}_{\mathbf{Y},ic}$; and (2) overcoming the invertibility limitation of the estimated precision matrix, the L_2 penalty term is added to mathematical programming (5) by taking the idea of ridge panelized likelihood ratio (RPLR) procedure. Based on this procedure, the precision matrix of high-dimensional process under measurement errors denoted by $\hat{\boldsymbol{\Omega}}_t^{RPLRME}$ can be estimated as:

$$\hat{\boldsymbol{\Omega}}_t^{RPLRME} = \arg\min_{\boldsymbol{\Omega}} \left\{ tr(\boldsymbol{\Omega}\mathbf{S}_t) - \log|\boldsymbol{\Omega}| + \frac{\theta}{2}\|\boldsymbol{\Omega} - \boldsymbol{\Omega}_{ic}\| \right\} \quad (6)$$

where $\boldsymbol{\Omega}_{ic} = \boldsymbol{\Sigma}_{\mathbf{Y},ic}^{-1}$ and $\theta; \theta > 0$ is a tuning parameter which is employed to obtain various levels of shrinkage of $\hat{\boldsymbol{\Omega}}_t^{RPLRME}$. Based on the mathematical programming (6), $\hat{\boldsymbol{\Omega}}_t^{RPLRME}$ can be attained according to Equation (7).

$$\hat{\boldsymbol{\Omega}}_t^{RPLRME} = \left\{ \left(\theta \mathbf{I}_p + \frac{1}{4}\left(\mathbf{S}_t - \theta \boldsymbol{\Omega}_{ic}\right)^2 \right)^{\frac{1}{2}} + \frac{1}{2}\left(\mathbf{S}_t - \theta \boldsymbol{\Omega}_{ic}\right) \right\}^{-1} \tag{7}$$

It can be concluded from Equation (7) that $\hat{\boldsymbol{\Omega}}_t^{RPLRME}$ tends toward $\boldsymbol{\Omega}_{ic}$ when $\theta \to \infty$ while in situation that $\theta \to 0$, $\hat{\boldsymbol{\Omega}}_t^{RPLRME}$ approaches $\mathbf{S}_t^{-1}$. Determining the status of high-dimensional process variability under gauge measurement errors is equivalent to conducting the following hypothesis test:

$$\begin{aligned} H_0 &: \boldsymbol{\Sigma}_{\mathbf{Y}} = \mathbf{B}\boldsymbol{\Sigma}_{\mathbf{X},ic}\mathbf{B}^T + \boldsymbol{\Sigma}_{\boldsymbol{\varepsilon}} \\ H_1 &: \boldsymbol{\Sigma}_{\mathbf{Y}} \neq \mathbf{B}\boldsymbol{\Sigma}_{\mathbf{X},ic}\mathbf{B}^T + \boldsymbol{\Sigma}_{\boldsymbol{\varepsilon}} \end{aligned} \tag{8}$$

For t^{th} random sample, the developed statistic based on the integration of the ridge penalized likelihood ratio estimator and the measurement errors (RPLRME) can be written as:

$$RPLRME_t = tr\left(\boldsymbol{\Omega}_{ic}\mathbf{S}_t\right) + \ln\left|\hat{\boldsymbol{\Omega}}_t^{RPLRME}\right| - \ln\left|\boldsymbol{\Omega}_{ic}\right| - tr\left(\hat{\boldsymbol{\Omega}}_t^{RPLRME}\mathbf{S}_t\right) \tag{9}$$

The RPLRME chart issues an out-of-control signal whenever $RPLRME_t > UCL_{RPLRME}$ where the value of UCL_{RPLRME} is selected so that the in-control average run length (ARL_{ic}) be equal to $\frac{1}{\alpha}$. Note that the average run length is defined as the expected value of a run length random variable which specifies the number of samples till issuing an out-of-control signal.

3. RPLRME Control Chart Under Multiple Measurements Approach

In order to increase the chart detectability and get more robust results, the undesired impact of gauge imprecision should be diminished by employing remedial approaches. In this regard, multiple measurements strategy as one of the most efficient remedial methods was proposed by [27] and has been employed in some other studies such as [28-30]. Taking multiple measurements on each sampled point instead of individual ones enhances the chart sensitivity due to reduction of the extra variability caused by error term. Based on this, a novel control chart hereafter called RPLRMME is established by extending the RPLRME chart under multiple measurements strategy. Let $\bar{\mathbf{Y}}_t = (\bar{\mathbf{y}}_{t1}, \bar{\mathbf{y}}_{t2}, ..., \bar{\mathbf{y}}_{tn})_{p\times n}$ denotes the observations taken at the t^{th} subgroup where each sample unit is inspected $m; m > 1$ times. Besides, $\bar{\mathbf{y}}_{ti} = (\bar{y}_{ti1}, \bar{y}_{ti2}, ..., \bar{y}_{tip})^T$ represents the elements of the i^{th} column of observations matrix $\bar{\mathbf{Y}}_t$ where $\bar{y}_{tij} = \frac{\sum_{r=1}^{m} y_{tijr}}{m}$. It can be statistically checked that $\bar{\mathbf{y}}_{ti}$ follows a p-variate normal distribution with mean vector $\boldsymbol{\mu}_{\bar{\mathbf{Y}}} = \mathbf{A} + \mathbf{B}\boldsymbol{\mu}_{\mathbf{X}}$ and covariance matrix $\boldsymbol{\Sigma}_{\bar{\mathbf{Y}}} = \mathbf{B}\boldsymbol{\Sigma}_{\mathbf{X}}\mathbf{B}^T + \frac{\boldsymbol{\Sigma}_{\boldsymbol{\varepsilon}}}{m}$. Accordingly, the covariance matrix of $\bar{\mathbf{y}}_{ti}$ can be rewritten as:

$$\boldsymbol{\Sigma}_{\bar{\mathbf{Y}}} = \begin{pmatrix} b_1^2\sigma_{11} + \frac{\sigma_{\varepsilon,1}^2}{m} & b_1 b_2 \sigma_{12} & \cdots & b_1 b_p \sigma_{1p} \\ b_2 b_1 \sigma_{12} & b_2^2\sigma_{22} + \frac{\sigma_{\varepsilon,2}^2}{m} & \cdots & b_2 b_p \sigma_{2p} \\ \vdots & \vdots & \ddots & \vdots \\ b_p b_1 \sigma_{1p} & b_2 b_p \sigma_{2p} & \cdots & b_p^2\sigma_{pp} + \frac{\sigma_{\varepsilon,p}^2}{m} \end{pmatrix}_{p\times p} \tag{10}$$

The likelihood function under taking m measurements on each sampled item is constructed by replacing $\mathbf{y}_{ti}$ by $\bar{\mathbf{y}}_{ti}$ in Equation (4). For t^{th} random sample, the estimation of precision matrix to construct the RPLEMME chart is:

$$\hat{\boldsymbol{\Omega}}_t^{RPLRMME} = \underset{\boldsymbol{\Omega}}{\arg\min}\left\{ tr\left(\boldsymbol{\Omega}\mathbf{S}_t^m\right) - \log\left|\boldsymbol{\Omega}\right| + \frac{\theta}{2}\left\|\boldsymbol{\Omega} - \boldsymbol{\Omega}_{ic}^m\right\|\right\} \quad (11)$$

where $\mathbf{S}_t^m = \frac{1}{n}\sum_{i=1}^{n}\left(\bar{\mathbf{y}}_{ti} - \boldsymbol{\mu}_{\bar{Y}}\right)\left(\bar{\mathbf{y}}_{ti} - \boldsymbol{\mu}_{\bar{Y}}\right)^T$.

Equivalently, we can write:

$$\hat{\boldsymbol{\Omega}}_t^{RPLRMME} = \left\{\left(\theta\mathbf{I}_p + \frac{1}{4}\left(\mathbf{S}_t^m - \theta\boldsymbol{\Omega}_{ic}^m\right)^2\right)^{\frac{1}{2}} + \frac{1}{2}\left(\mathbf{S}_t^m - \theta\boldsymbol{\Omega}_{ic}^m\right)\right\}^{-1} \quad (12)$$

Using RPLRMME chart for Phase II monitoring of high-dimensional process variability is equivalent to test the null hypothesis $H_0 : \boldsymbol{\Sigma}_{\bar{\mathbf{Y}}} = \mathbf{B}\boldsymbol{\Sigma}_0\mathbf{B}^T + \frac{\boldsymbol{\Sigma}_\varepsilon}{m}$ versus the alternative one $H_1 : \boldsymbol{\Sigma}_{\bar{\mathbf{Y}}} \neq \mathbf{B}\boldsymbol{\Sigma}_0\mathbf{B}^T + \frac{\boldsymbol{\Sigma}_\varepsilon}{m}$. The developed chart statistic at the t^{th} sampling stage is given as:

$$RPLRMME_t = tr\left(\boldsymbol{\Omega}_{ic}^m\mathbf{S}_t^m\right) + \ln\left|\hat{\boldsymbol{\Omega}}_t^{RPLRMME}\right| - \ln\left|\boldsymbol{\Omega}_{ic}^m\right| - tr\left(\hat{\boldsymbol{\Omega}}_t^{RPLRMME}\mathbf{S}_t^m\right) \quad (13)$$

A signal is triggered by The RPLRMME if $RPLRMME_t > UCL_{RPLRMME}$ where the value of $UCL_{RPLRMME}$ is set based on simulation experiments to achieve a pre-determined ARL_{ic} .

4. Performance Comparison

In this section, the impact of inaccurate measurements on efficiency of the RPLR chart is investigated based on Monte Carlo simulations. Consider a multivariate process in which the product quality is characterized via $p = 10$ normally distributed variables. It is assumed that $\boldsymbol{\Sigma}_{\mathbf{X},ic} = \mathbf{I}_{10}$ when the process is in-control. The parameters of the RPLRME chart are selected as $n = 5$ and $\theta = 10$. We consider an additive covariate model with constant values of $\mathbf{A} = \mathbf{0}_{10\times 1}$ and $\mathbf{B} = \mathbf{I}_{10}$ in which $\sigma_{\varepsilon,j}^2 = \sigma_\varepsilon^2; \sigma_\varepsilon^2 \in \{0, 0.05, 0.1, 0.15, 0.2, 0.25\}$ for $j = 1,...,10$. It is worth mentioning that the case $\sigma_\varepsilon^2 = 0$ implies that the observations are collected under without measurement errors condition. For each value of σ_ε^2 , the $UCL_{RPLRMME}$ is set subject to $ARL_{ic} = 200$. Then, the sensitivity of the RPLRME chart under seven out-of-control scenarios is evaluated in terms of ARL_{oc} and $SDRL_{oc}$. These scenarios include diagonal, off-diagonal as well as concurrent diagonal/off-diagonal disturbances as follows:

Scenario 1: The occurrence of assignable cause leads to shifts in all covariance matrix elements as follows:

$$\sigma_j^2 = 1 + \delta^2; j = 1,...,10 \text{ and } \sigma_{jk} = \delta; j,k = 1,...,10 \ \& \ j \neq k \quad (14)$$

Scenario 2: The second out-of-control scenario is similar to the first scenario with this difference that the assignable cause affects the variance and covariance elements of the first five variables.

$$\sigma_j^2 = 1 + \delta^2; j = 1,...,5 \text{ and } \sigma_{jk} = \delta; j,k = 1,...,5 \ \& \ j \neq k \quad (15)$$

Scenario 3: In this condition, the variance and covariance elements of the first and second variables are affected as Equation (16):

$$\sigma_j^2 = 1 + \delta^2; j = 1,2 \text{ and } \sigma_{12} = \sigma_{21} = \delta \quad (16)$$

Scenario 4: As given in Equation (17), the occurrence of assignable cause affects all variance elements while the covariance elements remain unchanged.

$$\sigma_j^2 = 1 + \delta^2; j = 1,...,10 \quad (17)$$

Scenario 5: The out-of-control condition is restricted to only the variance of the first variable. In other words, the other 99 variance/covariance elements remain unchanged:

$$\sigma_1^2 = 1 + \delta^2 \quad (18)$$

Scenario 6: As seen in Equation (19), the out-of-control covariance matrix includes off-diagonal disturbances related to the first five variables.

$$\sigma_{jk} = \delta; j,k = 1,...,5 \ \& \ j \neq k \quad (19)$$

Scenario 7: This scenario is similar to the previous scenario with this difference that the assignable cause changes the covariance of the first and second variables.

$$\sigma_{12} = \sigma_{21} = \delta \quad (20)$$

The resulting *ARL*s and *SDRL*s of the developed RPLRME chart for both with and without error cases under the mentioned out-of-control scenarios when $\delta \in \{0, 0.1, 0.2, 0.3, 0.5, 0.75, 1\}$ are presented in Tables 2-8. As seen from Tables 2-8, the gauge measurement errors diminishes the detecting capability of the developed RPLRME chart to react to the sustained changes in covariance matrix elements. It can be confirmed from Tables 2-8 that the *ARL* and *SDRL* values increase as the error variance increases. That is to say that the larger value of σ_ε^2, the larger values of both ARL_{oc} and $SDRL_{oc}$. Specifically, it can be observed from Table 2 that for $\delta = 0.1$, the chart obtains $ARL_{oc} = 71.8085$ when the measurements are accurate. However, the existence of measurement errors increases the value of ARL_{oc} to 78.2490, 84.9975, 89.4355, 95.9365, and 96.1550 when σ_ε^2 equals to 0.05, 0.1, 0.15, 0.2, and 0.25, respectively. In other words, for $\delta = 0.1$, increasing the error variance to 0.05, 0.1, 0.15, 0.2, and 0.25 leads to reducing the chart sensitivity about 8.97, 18.37, 24.55, 33.60, and 33.90 percent, respectively, when the covariance matrix elements are affected according to the first out-of-control scenario. The results of Table 3 indicate that both the values of ARL_{oc} and $SDRL_{oc}$ in scenario 2 are always larger than those of scenario 1. This is due to the fact that, in spite of the first scenario, the assignable cause affects 25 percent of the covariance matrix elements in the second scenario. For instance under the second scenario, when $\sigma_\varepsilon^2 = 0.1$ and $\delta = 0.3$, the developed chart obtains $ARL_{oc} = 41.1420$ which is remarkably larger than that of the first scenario, i.e. $ARL_{oc} = 9.8935$. It can be also concluded from comparing the results of Tables 2-4 that the capability of the developed chart to detect covariance matrix anomalies significantly reduces when the assignable cause affects the process variability according to the third out-of-control scenario.

Table 5 reveals that as the error variance increases from 0 to 0.25, the efficiency of the RPLRME control chart to detect diagonal covariance matrix shifts reduces, dramatically. For instance, for $\delta = 0.5$, increasing the error variance from 0.05 to 0.25 result in increasing the value of ARL_{oc} from 14.3550 to 18.7240. That is to say, under the mentioned condition, the detection capability of the RPLRME chart degrades about 30.43 percent. Besides, the impact of off-diagonal shifts on detection performance of the developed chart can be disclosed by comparing the results of Tables 2 and 5. For more clarification, under the case $\sigma_\varepsilon^2 = 0.1$ when $\delta = 0.5$, we have $ARL_{oc} = 3.6375$ when both diagonal and off-diagonal are affected by the assignable cause while the RPLRME chart detects the sustained shift in diagonal elements after average of 15.5630 samples. The results of Tables 6 and 8 tells us that in contrast to the other charts developed for monitoring high-dimensional processes, the proposed RPLRME scheme can detect sparse shifts when only few number of covariance matrix elements are changed. However, as expected, the occurrence of such shifts is detected with a delay when the magnitude of shift is small. It is clear from the values of *ARL*s and *SDRL*s shown in Table 7 that similar to the previous out-of-control scenarios, the existence of measurement error causes a delay in the detection of shift when only off-diagonal elements change from their nominal values.

Tab. 2. ARL and SDRL comparison under different error variance values in scenario 1

δ	Criterion	UCL_{RPLRME}					
		4.8104	5.1018	5.3913	5.6462	5.8613	6.0642
		$\sigma_\varepsilon^2 = 0$	$\sigma_\varepsilon^2 = 0.05$	$\sigma_\varepsilon^2 = 0.1$	$\sigma_\varepsilon^2 = 0.15$	$\sigma_\varepsilon^2 = 0.2$	$\sigma_\varepsilon^2 = 0.25$
0	*ARL*	200.0270	200.3655	200.6080	200.2390	200.0824	199.2450
	SDRL	198.3768	202.8921	203.3510	199.1435	202.0609	202.5535
0.1	*ARL*	71.8085	78.2490	84.9975	89.4355	95.9365	96.1550
	SDRL	69.2305	75.6523	83.7848	87.6284	95.5930	97.5912

0.2	*ARL*	18.9235	21.1540	23.9755	24.8830	28.4755	30.4290
	SDRL	18.5084	20.5907	22.9208	24.2471	28.5526	30.4888
0.3	*ARL*	7.9315	8.6975	9.8935	10.9760	12.0225	13.4650
	SDRL	7.5446	8.3050	9.8936	10.4862	11.4784	12.8001
0.50	*ARL*	3.2080	3.3755	3.6375	3.9580	4.0320	4.5755
	SDRL	2.6986	2.9492	3.0089	3.3062	3.4802	3.9587
0.75	*ARL*	1.7765	1.8815	1.9365	2.0780	2.1435	2.2315
	SDRL	1.2285	1.2966	1.4041	1.4846	1.5672	1.6713
1	*ARL*	1.3030	1.3510	1.4155	1.4745	1.4895	1.5155
	SDRL	0.6176	0.7043	0.7518	0.8501	0.8504	0.8923

Tab. 3. ARL and SDRL comparison under different error variance values in scenario 2

δ	Criterion	UCL_{RPLRME}					
		4.8104	5.1018	5.3913	5.6462	5.8613	6.0642
		$\sigma_\varepsilon^2 = 0$	$\sigma_\varepsilon^2 = 0.05$	$\sigma_\varepsilon^2 = 0.1$	$\sigma_\varepsilon^2 = 0.15$	$\sigma_\varepsilon^2 = 0.2$	$\sigma_\varepsilon^2 = 0.25$
0	*ARL*	200.0270	200.3655	200.6080	200.2390	200.0824	199.2450
	SDRL	198.3768	202.8921	203.3510	199.1435	202.0609	202.5535
0.1	*ARL*	151.7150	152.8570	158.2295	159.8290	160.9275	165.6505
	SDRL	156.9350	152.4835	154.4426	160.0299	160.4088	162.3510
0.2	*ARL*	73.4590	77.5315	84.9070	86.7075	94.6700	97.8320
	SDRL	75.5450	78.4171	82.8794	87.7331	95.1895	97.7902
0.3	*ARL*	33.2720	36.4045	41.1420	43.0160	46.2385	49.7135
	SDRL	33.1084	34.3605	40.1299	41.8369	46.8872	49.5135
0.5	*ARL*	10.2085	10.6500	12.3230	13.5325	14.4355	15.7470
	SDRL	9.6701	10.5633	11.9362	13.7195	13.7217	14.8825
0.75	*ARL*	3.9700	4.4025	4.5290	5.1435	5.5450	5.7540
	SDRL	3.3421	3.9340	4.1704	4.6375	4.9773	5.0501
1	*ARL*	2.2880	2.4870	2.5055	2.6805	2.8160	3.0440
	SDRL	1.7273	1.9702	1.9774	2.0299	2.2380	2.5104

Tab. 4. ARL and SDRL comparison under different error variance values in scenario 3

δ	Criterion	UCL_{RPLRME}					
		4.8104	5.1018	5.3913	5.6462	5.8613	6.0642
		$\sigma_\varepsilon^2 = 0$	$\sigma_\varepsilon^2 = 0.05$	$\sigma_\varepsilon^2 = 0.1$	$\sigma_\varepsilon^2 = 0.15$	$\sigma_\varepsilon^2 = 0.2$	$\sigma_\varepsilon^2 = 0.25$
0	*ARL*	200.0270	200.3655	200.6080	200.2390	200.0824	199.2450
	SDRL	198.3768	202.8921	203.3510	199.1435	202.0609	202.5535
0.1	*ARL*	182.4620	189.9020	191. 1520	192.2425	193.5325	194.8600
	SDRL	177.0263	184.1790	191. 2818	192.2316	194.6210	194.7752
0.2	*ARL*	167.4450	168.2690	170.4525	172.6790	174.1975	175.1330
	SDRL	167.1549	168.0785	168.1042	172.6253	174.1035	174.3643
0.3	*ARL*	134.4550	135.1255	137.6800	140.4765	142.0880	143.0055
	SDRL	131.0360	135.3170	138.0111	142.3586	140.4695	141.4138
0.50	*ARL*	62.5985	64.9740	71.8440	74.7880	75.4545	78.3770
	SDRL	64.5629	64.7282	70.1587	74.9071	75.5362	79.3273
0.75	*ARL*	23.3575	24.8950	27.0560	28.9930	30.9645	32.3025
	SDRL	22.7927	24.6502	26.9691	28.8862	30.0898	31.9370
1	*ARL*	9.1005	10.0330	10.6560	11.6480	12.7095	13.9965
	SDRL	8.6486	9.5330	9.9441	10.8227	12.4205	13.3382

Tab. 5. ARL and SDRL comparison under different error variance values in scenario 4

δ	Criterion	UCL_{RPLRME}					
		4.8104	5.1018	5.3913	5.6462	5.8613	6.0642
		$\sigma_\varepsilon^2 = 0$	$\sigma_\varepsilon^2 = 0.05$	$\sigma_\varepsilon^2 = 0.1$	$\sigma_\varepsilon^2 = 0.15$	$\sigma_\varepsilon^2 = 0.2$	$\sigma_\varepsilon^2 = 0.25$
0	*ARL*	200.0270	200.3655	200.6080	200.2390	200.0824	199.2450
	SDRL	198.3768	202.8921	203.3510	199.1435	202.0609	202.5535
0.1	*ARL*	181.3370	183.9370	184.1130	185.3660	186.0315	187.4475

	SDRL	184.0674	184.4873	184.7206	185.5717	185.3361	187.5506
0.2	*ARL*	112.3760	118.1060	121.7320	121.89085	122.5630	123.8915
	SDRL	111.1317	118.6844	117.1182	123.3894	122.9964	123.4841
0.3	*ARL*	61.3020	61.8475	66.8410	69.9680	70.2390	70.8125
	SDRL	61.0218	61.8580	65.4398	69.6326	70.5960	70.6627
0.50	*ARL*	13.4815	14.3550	15.5630	16.6285	17.3055	18.7240
	SDRL	12.8838	14.3760	15.1277	16.3202	17.5520	18.4422
0.75	*ARL*	2.7455	2.9370	3.1570	3.3265	3.5515	3.8760
	SDRL	2.1310	2.4333	2.6015	2.9078	2.9405	3.3017
1	*ARL*	1.2635	1.3225	1.3535	1.4650	1.4740	1.5370
	SDRL	0.5632	0.6471	0.6977	0.8081	0.8314	0.8860

Tab. 6. ARL and SDRL comparison under different error variance values in scenario 5

δ	Criterion	UCL_{RPLRME}					
		4.8104	5.1018	5.3913	5.6462	5.8613	6.0642
		$\sigma_\varepsilon^2 = 0$	$\sigma_\varepsilon^2 = 0.05$	$\sigma_\varepsilon^2 = 0.1$	$\sigma_\varepsilon^2 = 0.15$	$\sigma_\varepsilon^2 = 0.2$	$\sigma_\varepsilon^2 = 0.25$
0	*ARL*	200.0270	200.3655	200.6080	200.2390	200.0824	199.2450
	SDRL	198.3768	202.8921	203.3510	199.1435	202.0609	202.5535
0.1	*ARL*	193.0845	194.5760	196.0710	197.3380	197.9020	198.1715
	SDRL	193.3813	194.6717	197.0311	196.1353	196.4102	196.2692
0.2	*ARL*	190.5070	192.4800	192.6140	193.4525	194.0840	194.8685
	SDRL	190.1296	192.7278	192.8264	193.8498	194.8616	193.0579
0.3	*ARL*	172.3015	175.3870	176.4730	176.6070	177.6580	178.3040
	SDRL	172.2264	172.4015	177.3245	177.5226	177.9541	178.8112
0.50	*ARL*	131.0185	133.5100	135.3715	140.7375	141.9195	142.1545
	SDRL	128.4163	135.2401	135.4230	140.4510	141.8828	141.9179
0.75	*ARL*	75.2030	77.8200	80.5470	81.7215	85.1150	86.7445
	SDRL	74.9936	76.8780	80.6289	81.9079	86.6554	86.7219
1	*ARL*	33.0060	34.8290	37.5640	42.2255	43.5820	44.7785
	SDRL	32.8341	33.2356	37.4780	42.4154	42.5298	43.7556

Tab. 7. ARL and SDRL comparison under different error variance values in scenario 6

δ	Criterion	UCL_{RPLRME}					
		4.8104	5.1018	5.3913	5.6462	5.8613	6.0642
		$\sigma_\varepsilon^2 = 0$	$\sigma_\varepsilon^2 = 0.05$	$\sigma_\varepsilon^2 = 0.1$	$\sigma_\varepsilon^2 = 0.15$	$\sigma_\varepsilon^2 = 0.2$	$\sigma_\varepsilon^2 = 0.25$
0	*ARL*	200.0270	200.3655	200.6080	200.2390	200.0824	199.2450
	SDRL	198.3768	202.8921	203.3510	199.1435	202.0609	202.5535
0.1	*ARL*	161.5690	163.1995	165.1805	167.5415	169.2515	173.2880
	SDRL	161.0361	161.1632	165.0655	165.9218	169.7752	170.2243
0.2	*ARL*	92.9490	97.9600	100.8430	108.2135	111.6610	116.5050
	SDRL	90.7152	94.7094	102.5694	110.6930	112.0497	119.9457
0.3	*ARL*	47.3150	51.8035	56.3675	63.0490	70.0625	70.6720
	SDRL	45.5090	51.2175	54.2517	60.3571	70.5067	71.1131
0.50	*ARL*	16.9195	18.9950	21.6200	23.5730	25.8125	29.3475
	SDRL	16.5987	17.9258	20.9726	21.9843	24.7490	28.3228
0.75	*ARL*	7.9120	8.7765	9.5920	10.8185	11.6465	12.9700
	SDRL	7.4869	8.5333	9.0608	10.2250	11.6724	12.5675
1	*ARL*	4.8110	5.3605	5.9730	6.3250	6.6520	7.4070
	SDRL	4.3165	4.8903	5.6324	5.7195	6.1936	6.7696

Tab. 8. ARL and SDRL comparison under different error variance values in scenario 7

δ	Criterion	UCL_{RPLRME}					
		4.8104	5.1018	5.3913	5.6462	5.8613	6.0642
		$\sigma_\varepsilon^2 = 0$	$\sigma_\varepsilon^2 = 0.05$	$\sigma_\varepsilon^2 = 0.1$	$\sigma_\varepsilon^2 = 0.15$	$\sigma_\varepsilon^2 = 0.2$	$\sigma_\varepsilon^2 = 0.25$
0	*ARL*	200.0270	200.3655	200.6080	200.2390	200.0824	199.2450
	SDRL	198.3768	202.8921	203.3510	199.1435	202.0609	202.5535

0.1	*ARL*	194.6415	195.6575	196. 3930	197.3485	198.6540	198.8185
	SDRL	194.8101	195.0791	196.1245	196.7619	197.5123	198.4807
0.2	*ARL*	186.2280	187.0325	187.6900	188.8865	190.4890	193.1945
	SDRL	187.8216	188.0193	188.0547	188.3663	188.1223	193.2670
0.3	*ARL*	175.7235	176.3475	177.5375	177.6245	178.0000	180.5335
	SDRL	172.5511	173.0896	176.6114	177.9696	180.3428	185.6862
0.5	*ARL*	127.3435	128.7440	138.7395	139.1250	139.5340	142.5995
	SDRL	124.6256	127.2070	135.4627	136.2119	137.9397	144.8344
0.75	*ARL*	80.9620	88.3155	93.7785	99.0500	106.7805	108.0015
	SDRL	75.2710	88.9093	89.6775	100.4935	104.9576	106.1982
1	*ARL*	55.9760	57.9725	64.5650	69.7905	70.2505	78.9680
	SDRL	56.2406	57.3907	60.9027	68.0019	68.1556	79.3262

In the rest of this section, according to section 3, we explore the performance of the RPLRMME chart in reducing the undesired impact of error contamination. We employ simulation experiments considering the same defined out-of-control scenarios when $\sigma_\varepsilon^2 = 0.25$. For this purpose, the performance of the RPLRME chart is compared to RPLRMME chart with $m = 2,3,5$ measurements per item in terms of *ARL* and *SDRL* and the results are summarized in Tables 9-15. The results reveal the superiority of the RPLRMME chart over the RPLRME one for both sparse or non-sparse shift patterns. That is to say, the delay in detection of sustained shifts caused by the error contamination can be adequately reduced when each item is measured several times. For more clarification, Figure 1 illustrates the percentage of *ARL* deterioration of the RPLRMME chart with $m = 1,2,3$ and 5 under the first out-of-control scenario for $\delta \in \{0.1, 0.2, 0.3, 0.5, 0.75, 1\}$. For instance, in this scenario when $\delta = 0.5$, the *ARL* obtained by the RPLRMME chart with $m = 5$ is only 3.634663 percent larger than that of the no-error case. However, under single measurement condition, the mentioned difference increases to 42.62781 percent. This trend can be also observed for the other out-of-control scenarios. Besides, as indicated, the difference between with and without-error cases diminishes as the number of measurements per sampled item increases. In other words, for large values of m , the *ARL* values approach those obtained under no-error cases. The results of Tables 9-15 tell us that the run length properties of the RPLRMME chart with $m = 5$ inspections per sampled unit is approximately similar to those of no-error case. The same conclusions can be drawn when *SDRL* metric is taken into account.

Tab. 9. ARL and SDRL values when $\sigma_\varepsilon^2 = 0.25$ and $m \in \{1,2,3,5\}$ in scenario 1

δ	Criterion	$UCL_{RPLRMME}$				
		4.8104	6.0642	5.5185	5.2926	5.0970
		No error	$m = 1$	$m = 2$	$m = 3$	$m = 5$
0	*ARL*	200.0270	199.2450	201.8091	199.0165	199.4916
	SDRL	198.3768	202.5535	199.1630	192.9853	197.2154
0.1	*ARL*	71.8085	96.1550	86.6425	81.5708	77.1850
	SDRL	69.2305	97.5912	87.4703	79.9065	76.7903
0.2	*ARL*	18.9235	30.4290	24.8424	22.1050	20.9198
	SDRL	18.5084	30.4888	24.2118	21.1159	20.5495
0.3	*ARL*	7.9315	13.4650	10.0922	9.3222	8.8524
	SDRL	7.5446	12.8001	9.5824	8.8027	8.3229
0.50	*ARL*	3.2080	4.5755	3.7839	3.5960	3.3246
	SDRL	2.6986	3.9587	3.2522	3.0572	2.7306
0.75	*ARL*	1.7765	2.2315	2.0240	1.9196	1.8548
	SDRL	1.2285	1.6713	1.4184	1.3039	1.2758
1	*ARL*	1.3030	1.5155	1.4167	1.4072	1.3562
	SDRL	0.6176	0.8923	0.7645	0.7402	0.6927

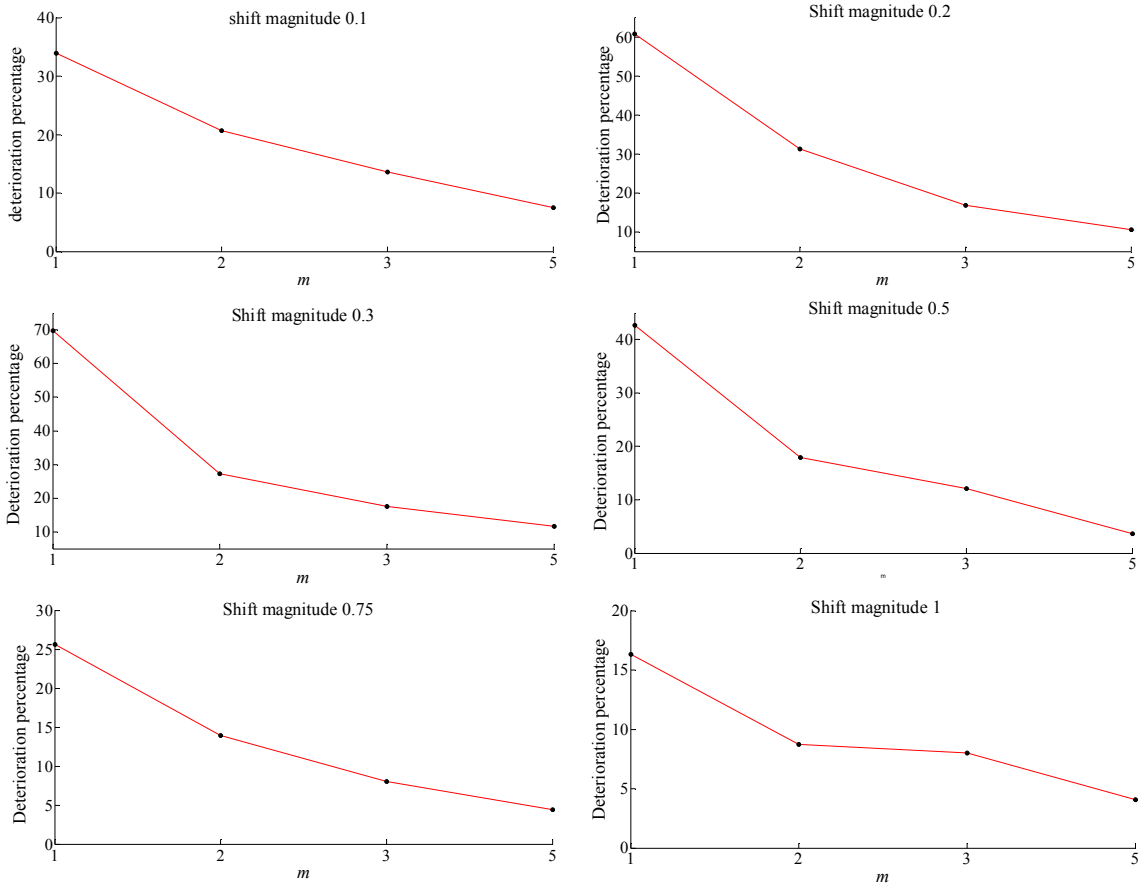

Fig. 1. Percentage of ARL deterioration in scenario 1

Tab. 10. ARL and SDRL values when $\sigma_\varepsilon^2 = 0.25$ and $m \in \{1,2,3,5\}$ in scenario 2

δ	Criterion	UCL_{RPLRME}				
		4.8104	6.0642	5.5185	5.2926	5.0970
		No error	$m = 1$	$m = 2$	$m = 3$	$m = 5$
0	*ARL*	200.0270	199.2450	201.8091	199.0165	199.4916
	SDRL	198.3768	202.5535	199.1630	192.9853	197.2154
0.1	*ARL*	151.7150	165.6505	158.3782	153.7458	152.4110
	SDRL	156.9350	162.3510	157.8713	153.9333	151.4356
0.2	*ARL*	73.4590	97.8320	84.5340	79.8732	75.9162
	SDRL	75.5450	97.7902	83.4444	78.5593	74.7028
0.3	*ARL*	33.2720	49.7135	42.8334	39.3472	36.7922
	SDRL	33.1084	49.5135	42.6793	39.0212	36.3339
0.50	*ARL*	10.2085	15.7470	12.6740	11.8168	10.8622
	SDRL	9.6701	14.8825	12.2175	11.6006	10.2842
0.75	*ARL*	3.9700	5.7540	4.7766	4.4780	4.3406
	SDRL	3.3421	5.0501	4.2139	3.9376	3.8650
1	*ARL*	2.2880	3.0440	2.5774	2.4630	2.3534
	SDRL	1.7273	2.5104	1.9762	1.9489	1.7913

Tab. 11. ARL and SDRL values when $\sigma_\varepsilon^2 = 0.25$ and $m \in \{1,2,3,5\}$ in scenario 3

δ	Criterion	UCL_{RPLRME}				
		4.8104	6.0642	5.5185	5.2926	5.0970
		No error	$m=1$	$m=2$	$m=3$	$m=5$
0	*ARL*	200.0270	199.2450	201.8091	199.0165	199.4916
	SDRL	198.3768	202.5535	199.1630	192.9853	197.2154
0.1	*ARL*	182.4620	194.8600	188.2894	193.7182	189.7958
	SDRL	177.0263	194.7752	186.8011	196.6489	189.5215
0.2	*ARL*	167.4450	175.1330	168.8866	167.0454	165.2840
	SDRL	167.1549	174.3643	172.8312	167.7489	168.3092
0.3	*ARL*	134.4550	143.0055	137.7388	131.2532	130.4826
	SDRL	131.0360	141.4138	138.1823	132.2029	131.7868
0.50	*ARL*	62.5985	78.3770	73.1550	67.8338	65.9210
	SDRL	64.5629	79.3273	71.1708	66.3890	65.5718
0.75	*ARL*	23.3575	32.3025	27.8096	25.3058	24.6116
	SDRL	22.7927	31.9370	27.5751	25.2759	24.2312
1	*ARL*	9.1005	13.9965	11.4574	10.5152	9.8968
	SDRL	8.6486	13.3382	10.6726	9.9103	9.5027

Tab. 12. ARL and SDRL values when $\sigma_\varepsilon^2 = 0.25$ and $m \in \{1,2,3,5\}$ in scenario 4

δ	Criterion	UCL_{RPLRME}				
		4.8104	6.0642	5.5185	5.2926	5.0970
		No error	$m=1$	$m=2$	$m=3$	$m=5$
0	*ARL*	200.0270	199.2450	201.8091	199.0165	199.4916
	SDRL	198.3768	202.5535	199.1630	192.9853	197.2154
0.1	*ARL*	181.3370	187.4475	176.5550	176.4356	176.1178
	SDRL	184.0674	187.5506	176.9491	180.7028	179.2015
0.2	*ARL*	112.3760	123.8915	119.9202	115.9962	114.7818
	SDRL	111.1317	123.4841	119.8491	114.9623	116.0651
0.3	*ARL*	61.3020	70.8125	65.8958	65.6170	62.9370
	SDRL	61.0218	70.6627	65.1522	64.4477	60.6513
0.50	*ARL*	13.4815	18.7240	16.3666	14.6112	14.5450
	SDRL	12.8838	18.4422	15.8692	14.1536	14.1281
0.75	*ARL*	2.7455	3.8760	3.2512	3.1202	2.9294
	SDRL	2.1310	3.3017	2.6905	2.5754	2.3644
1	*ARL*	1.2635	1.5370	1.3878	1.3332	1.3272
	SDRL	0.5632	0.8860	0.7424	0.6520	0.6787

Tab. 13. ARL and SDRL values when $\sigma_\varepsilon^2 = 0.25$ and $m \in \{1,2,3,5\}$ in scenario 5

δ	Criterion	UCL_{RPLRME}				
		4.8104	6.0642	5.5185	5.2926	5.0970
		No error	$m=1$	$m=2$	$m=3$	$m=5$
0	*ARL*	200.0270	199.2450	201.8091	199.0165	199.4916
	SDRL	198.3768	202.5535	199.1630	192.9853	197.2154
0.1	*ARL*	193.0845	198.1715	198.6568	196.0188	197.0706
	SDRL	193.3813	196.2692	206.0462	198.4430	197.4494
0.2	*ARL*	190.5070	194.8685	189.0488	191.8264	184.3404
	SDRL	190.1296	193.0579	182.9238	192.5177	180.7635
0.3	*ARL*	172.3015	178.3040	181.2012	176.5138	177.4280
	SDRL	172.2264	178.8112	182.3975	176.9453	181.9473
0.50	*ARL*	131.0185	142.1545	139.4750	135.4668	135.0024

	SDRL	128.4163	141.9179	140.3504	135.1690	134.2531
0.75	*ARL*	75.2030	86.7445	81.7062	80.5364	75.5910
	SDRL	74.9936	86.7219	82.5199	78.6665	74.3763
1	*ARL*	33.0060	44.7785	39.1652	36.2046	35.0308
	SDRL	32.8341	43.7556	39.1977	35.3549	33.8459

Tab. 14. ARL and SDRL values when $\sigma_\varepsilon^2 = 0.25$ and $m \in \{1,2,3,5\}$ in scenario 6

δ	Criterion	UCL_{RPLRME}				
		4.8104	6.0642	5.5185	5.2926	5.0970
		No error	$m = 1$	$m = 2$	$m = 3$	$m = 5$
0	*ARL*	200.0270	199.2450	201.8091	199.0165	199.4916
	SDRL	198.3768	202.5535	199.1630	192.9853	197.2154
0.1	*ARL*	161.5690	173.2880	169.8004	166.4040	159.9754
	SDRL	161.0361	170.2243	170.2430	163.6367	160.6542
0.2	*ARL*	92.9490	116.5050	104.1308	97.7810	95.3758
	SDRL	90.7152	119.9457	103.0086	98.3814	95.3568
0.3	*ARL*	47.3150	70.6720	58.6210	55.0554	51.1696
	SDRL	45.5090	71.1131	58.9310	55.0585	49.8473
0.50	*ARL*	16.9195	29.3475	22.6900	20.7418	18.9808
	SDRL	16.5987	28.3228	22.1158	20.0225	18.2600
0.75	*ARL*	7.9120	12.9700	10.0642	9.4114	8.6334
	SDRL	7.4869	12.5675	9.4414	8.9387	8.1535
1	*ARL*	4.8110	7.4070	5.9632	5.4426	5.2198
	SDRL	4.3165	6.7696	5.4595	4.8168	4.6219

Tab. 15. ARL and SDRL values when $\sigma_\varepsilon^2 = 0.25$ and $m \in \{1,2,3,5\}$ in scenario 7

δ	Criterion	UCL_{RPLRME}				
		4.8104	6.0642	5.5185	5.2926	5.0970
		No error	$m = 1$	$m = 2$	$m = 3$	$m = 5$
0	*ARL*	200.0270	199.2450	201.8091	199.0165	199.4916
	SDRL	198.3768	202.5535	199.1630	192.9853	197.2154
0.1	*ARL*	194.6415	198.8185	200.7230	189.8260	194.4568
	SDRL	194.8101	198.4807	197.2272	191.9087	194.7432
0.2	*ARL*	186.2280	193.1945	184.8002	182.3852	182.4656
	SDRL	187.8216	193.2670	184.1209	187.3233	181.2584
0.3	*ARL*	175.7235	180.5335	173.3552	169.0096	179.0492
	SDRL	172.5511	185.6862	172.8763	170.4638	180.5072
0.50	*ARL*	127.3435	142.5995	137.9468	137.6036	126.4556
	SDRL	124.6256	144.8344	137.6460	138.4305	126.1620
0.75	*ARL*	80.9620	108.0015	96.6572	92.2376	86.0044
	SDRL	75.2710	106.1982	95.6434	93.0626	86.9232
1	*ARL*	55.9760	78.9680	66.6894	63.7292	57.9780
	SDRL	56.2406	79.3262	64.8023	63.0132	58.2197

5. Conclusions and Future Directions

In this paper, we proposed a novel control chart based on the ridge penalized likelihood ratio statistic for Phase II monitoring of high-dimensional process variability taking the gauge impression into account. In contrast to the other control charts for covariance matrix monitoring under high-dimensionality, the proposed control chart relaxes the sparsity assumption of the covariance matrix. It means that on one hand, the developed chart can be used for monitoring both sparse and non-sparse high-dimensional covariance matrix, on the other hand it can even detect sparce shifts in diagonal and/or off-diagonal covariance matrix elements. To compensate for the adverse effect of contamination due to the measurement errors, the RPLRME chart statistic was extended such that each item in a subgroup is inspected several times. To probe the efficiency of the proposed RPLRME chart, seven out-of-control scenarios including both sparse and non-sparse shifts in

high-dimensional covariance were defined. Then, extensive simulation studies in terms of the *ARL* and *SDRL* metrics were implemented to investigate how gauge inaccuracy deteriorates the sensitivity of the proposed chart in the detection of different anomalies in diagonal and/or off-diagonal elements. As expected, the results confirmed that the gauge's inability to accurately measure the process observations reduces the sensitivity of the developed control chart while employing multiple measurements approach can adequately compensate for the undesired impact of contaminated observations due to measurement errors. In other words, the detection capability of the developed RPLRMME chart approaches no-error case when the number of inspections per sampled item increases. The future studies can be extended in two directions: (1) developing control charts for monitoring the variability of the high-dimensional process with finite horizon productions, and (2) investigating the impact of estimation error on conditional *ARL* properties of the proposed RPLRME control chart.

References

[1] Lim, J., & Lee, S. Phase II monitoring of changes in mean from high dimensional data. *Applied Stochastic Models in Business and Industry*, Vol. 33, No. 6, (2017), pp. 626-639.

[2] Feng, L., Ren, H., & Zou, C. A setwise EWMA scheme for monitoring high-dimensional datastreams. *Random Matrices: Theory and Applications*, Vol. 9, No. 02, (2020), p. 2050004.

[3] Ebrahimi, S., Ranjan, C., & Paynabar, K. Monitoring and root-cause diagnostics of high-dimensional data streams. *Journal of Quality Technology*, Vol. 54, No. 1, (2021), pp. 20-43.

[4] Gunaratne, N. G. T., Abdollahian, M. A., Huda, S., & Yearwood, J. Exponentially weighted control charts to monitor multivariate process variability for high dimensions. *International Journal of Production Research*, Vol. 55, No. 17, (2017), pp. 4948-4962.

[5] Abdella, G. M., Kim, J., Kim, S., Al-Khalifa, K. N., Jeong, M. K., Hamouda, A. M., & Elsayed, E. A. An adaptive thresholding-based process variability monitoring. *Journal of Quality Technology*, Vol. 51, No. 3, (2019), pp. 242-256.

[6] Kim, J., Abdella, G. M., Kim, S., Al-Khalifa, K. N., & Hamouda, A. M. Control charts for variability monitoring in high-dimensional processes. Computers & Industrial Engineering, Vol. 130, (2019), pp. 309-316.

[7] Abdella, G. M., Maleki, M. R., Kim, S., Al-Khalifa, K. N., & Hamouda, A. M. S. Phase-I monitoring of high-dimensional covariance matrix using an adaptive thresholding LASSO rule. *Computers & Industrial* Engineering, Vol. 144, (2020), pp. 106465.

[8] Fan, J., Shu, L., Yang, A., & Li, Y. Phase I analysis of high-dimensional covariance matrices based on sparse leading eigenvalues. *Journal of Quality Technology*, Vol. 53, No. 4, (2021), pp. 333-346.

[9] Saemian, M., Salmasnia, A., & Maleki, M. R. A generalized multiple dependent state sampling chart based on ridge penalized likelihood ratio for high-dimensional covariance matrix monitoring. *Scientia Iranica*, In Press, (2023).

[10] Jafari, M., Maleki, M. R., & Salmasnia, A. A high-dimensional control chart for monitoring process variability under gauge imprecision effect. *Production Engineering*, Vol. 17, (2023), pp. 547-564.

[11] Salmasnia, A., Maleki, M. R., & Mirzaei, M. Double Sampling Adaptive Thresholding LASSO Variability Chart for Phase II Monitoring of High-Dimensional Data Streams. *Journal of Industrial Integration and Management*, In Press, (2023).

[12] Maleki, M. R., & Salmasnia, A. Joint Monitoring of Process Location and Dispersion Based on CUSUM Procedure and Generalized Likelihood Ratio in the Presence of Measurement Errors. *Quality*

and Reliability Engineering International, Vol. 33, No. 7, (2017), pp. 1485-1498.

[13] Salmasnia, A., Maleki, M. R., & Niaki, S. T. A. Remedial measures to lessen the effect of imprecise measurement with linearly increasing variance on the performance of the MAX-EWMAMS scheme. *Arabian Journal for Science and Engineering*, Vol. 43, No. 6, (2018), pp. 3151-3162.

[14] Khalafi, S., Salmasnia, A., & Maleki, M. R. Remedial approaches to decrease the effect of measurement errors on simple linear profile monitoring. *International Journal for Quality Research*, Vol. 14, No. 4, (2020).

[15] Nguyen, H. D., Tran, K. P., & Tran, K. D. The effect of measurement errors on the performance of the Exponentially Weighted Moving Average control charts for the Ratio of Two Normally Distributed Variables. *European Journal of Operational Research*, Vol. 293, No. 1, (2021), pp. 203-218.

[16] Saha, S., Khoo, M. B., Castagliola, P., & Haq, A. Side sensitive modified group runs charts with and without measurement errors for monitoring the coefficient of variation. *Quality and Reliability Engineering International*, Vol. 37, No. 2, (2021), pp. 598-617.

[17] Saemian, M., Maleki, M. R. Salmasnia, A. Performance of Max-HEWMAMS control chart for simultaneous monitoring of process mean and variability in the presence of measurement errors, *International Journal of Applied Decision Sciences*, In Press, (2022).

[18] Sabahno, H., Amiri, A., & Castagliola, P. Evaluating the effect of measurement errors on the performance of the variable sampling intervals Hotelling's T^2 control charts. *Quality and Reliability Engineering International*, Vol. 34, No. 8, (2018), pp. 1785-1799.

[19] Zaidi, F. S., Castagliola, P., Tran, K. P., & Khoo, M. B. C. Performance of the hotelling T^2 control chart for compositional data in the presence of measurement errors. *Journal of Applied Statistics*, Vol. 46, No. 14, (2019), pp. 2583-2602.

[20] Nguyen, Q. T., Giner-Bosch, V., Tran, K. D., Heuchenne, C., & Tran, K. P. One-sided variable sampling interval EWMA control charts for monitoring the multivariate coefficient of variation in the presence of measurement errors. *The International Journal of Advanced Manufacturing Technology*, Vol. 115, (2021), pp. 1821-1851.

[21] Maleki, M. R., Ghashghaei, R., & Amiri, A. Simultaneous monitoring of multivariate process mean and variability in the presence of measurement error with linearly increasing variance under additive covariate model (research note). *International Journal of Engineering*, Vol. 29, No. 4, (2016), pp. 514-523.

[22] Amiri, A., Ghashghaei, R., & Maleki, M. R. On the effect of measurement errors in simultaneous monitoring of mean vector and covariance matrix of multivariate processes. *Transactions of the Institute of Measurement and Control*, Vol. 40, No. 1, (2018), pp. 318-330.

[23] Zaidi, F. S., Castagliola, P., Tran, K. P., & Khoo, M. B. C. Performance of the MEWMA CoDa control chart in the presence of measurement errors. *Quality and Reliability Engineering International*, Vol. 36, No. 7, (2020), pp. 2411-2440.

[24] Ayyoub, H. N., Khoo, M. B., Lee, M. H., & Haq, A. Monitoring multivariate coefficient of variation with upward Shewhart and EWMA charts in the presence of measurement errors using the linear covariate error model. *Quality and Reliability Engineering International*, Vol. 37, No. 2, (2021), pp. 694-716.

[25] Yousefi, S., Maleki, M. R. Salmasnia, A. Kiani Anbohi, M. On the performance of multivariate homogeneously weighted moving average chart for monitoring the process mean in the presence of

measurement errors. *Journal of Advanced Manufacturing Systems*, Vol. 22, No. 01, (2023), pp. 27-40.

[26] Maleki, M. R., Amiri, A., & Castagliola, P. Measurement errors in statistical process monitoring: A literature review. *Computers & Industrial Engineering*, Vol. 103, (2017), pp. 316-329.

[27] Linna, K. W., & Woodall, W. H. Effect of measurement error on Shewhart control charts. *Journal of Quality Technology*, Vol. 33, No. 2, (2001), pp. 213-222.

[28] Ghashghaei, R., Bashiri, M., Amiri, A., & Maleki, M. R. Effect of measurement error on joint monitoring of process mean and variability under ranked set sampling. *Quality and Reliability Engineering International*, Vol. 32, No. 8, (2016), pp. 3035-3050.

[29] Noor-ul-Amin, M., Javaid, A., Hanif, M., & Dogu, E. Performance of maximum EWMA control chart in the presence of measurement error using auxiliary information. *Communications in Statistics-Simulation and Computation*, Vol. 51, No. 9, (2022), pp. 5482-5506.

[30] Maleki, M. R. Salmasnia, A., Yarmohammadi, S. The Performance of Triple Sampling $\bar{X}$ Control Chart with Measurement Errors, *Quality Technology & Quantitative Management*, Vol. 19, No. 5, (2022), pp. 587-604.

Follow this article at the following site:

Esmaeil Safikhani, Ali Salmasnia & Mohammad Reza Maleki: A ridge penalized likelihood ratio chart for phase II monitoring of high-dimensional process dispersion under measurement system inaccuracy. IJIEPR 2023; 34 (2) :1-17
URL: http://ijiepr.iust.ac.ir/article-1-1501-en.html